Simultaneous Grinding and Dissolution of TNT Solids in an Agitated Slurry

Patrick C. Gilcrease, Vincent G. Murphy, and Kenneth F. Reardon
Dept. of Chemical and Bioresource Engineering, Colorado State University, Fort Collins, CO 80523

In the slurry-phase bioremediation of soils contaminated with 2,4,6-trinitrotoluene (TNT) solids, TNT dissolution can be the rate-limiting step in the biodegradation process. To determine the effects of slurry concentration on solids dissolution, TNT particles were dissolved in a stirred vessel containing water and inert Teflon (PTFE) chips. For a constant agitator speed, the solid–liquid mass-transfer coefficient (k_L) decreased as the percentage of PTFE solids was increased. However, observed dissolution rates for TNT beads in agitated slurries were much higher than anticipated due to the grinding effect of PTFE chips. A size–mass balance was used to account for the grinding of TNT beads in these slurries; this same balance was then used to predict TNT dissolution rates. Slurry grinding was shown to be an important mechanism for enhancing the dissolution of TNT solids, and the size–mass balance was demonstrated to be an effective tool for modeling this process. These results have important implications for the bioremediation of TNT solids in soil slurry reactors.

Introduction

The extensive use of 2,4,6-trinitrotoluene (TNT) as a military explosive has resulted in soil and groundwater contamination at former manufacturing and loading sites (Rieger and Knackmuss, 1995). Due to the toxicity and environmental persistence of TNT, there is a need to remediate these areas. For soil treatment, bioremediation may offer a cost-effective alternative to conventional processes such as incineration (Rieger and Knackmuss, 1995). The bioremediation of TNT contaminated soils is complicated by the fact that TNT solids or "nuggets" may be present in the soil matrix. Field trials of bioremediation processes have shown that these nuggets are slow to degrade (R. Kaake, personal communication, 1996). In addition, laboratory studies have shown that dissolution can be the rate-limiting step in the biodegradation of TNT solids (Gilcrease et al., 1996; Gilcrease, 1997).

One system for soil bioremediation is the slurry reactor. In this process, contaminated soil is mixed with water and nutrients; a microbial inoculum can also be added, but often a degrading population is already present. For the bioremediation of soil containing TNT nuggets, slurry reactors may offer an advantage, since dissolution rates can be increased with agitation. Soil slurry reactors contain up to 50 wt. % solids, most of which are soil particles rather than TNT nuggets (U.S. EPA, 1995). Therefore, the effect of high solids concentrations on solid–liquid mass transfer is of practical interest for this system.

From previous investigations, we know that two separate, opposing mechanisms may influence solid–liquid mass transfer in an agitated slurry. In the first mechanism, the effective viscosity of the slurry increases with the solids concentration (Ishii and Zuber, 1979). This elevated viscosity leads to turbulence damping, and the solid–liquid mass-transfer coefficient (k_L) decreases for a given agitator speed (Kikuchi et al., 1987b). The second mechanism is associated with collisions during agitation between the dissolving particles and other solids present. If these collisions are forceful enough, the dissolving particles may break, and the surface area for mass transfer increases. Low-energy collisions tend to chip or abrade the outside surface of the dissolving particle (*attrition*), while massive impacts can completely disintegrate the particle (*breakage*) (Austin et al., 1984). The phenomena of particle abrasion in stirred vessels and slurry damping of k_L each

Correspondence concerning this article should be addressed to P. C. Gilcrease at this current address: Dept. of Chemical and Petroleum Engineering, University of Wyoming, P.O. Box 3295, Laramie, WY 82071.

have been investigated separately (Nienow and Conti, 1978; Conti and Nienow, 1980; Kikuchi et al., 1987b); however, a combined solid–liquid mass-transfer model that accounts for both particle breakage and turbulence damping was not available.

The objective of this study was to quantify the effects of particle breakage and turbulence damping on solid–liquid mass transfer (TNT dissolution) in an agitated slurry. To eliminate any sorption effects, mass-transfer experiments were conducted in slurries of inert, nonsorbing polytetrafluoroethylene (PTFE) boiling chips. This allowed for direct determination of the effect of slurry loading on $k_L a$. While the addition of PTFE solids decreased the mass-transfer coefficient, the TNT solid surface area (a) was enhanced due to TNT grinding associated with the PTFE slurry. This grinding resulted in a net positive effect of PTFE solids on the TNT dissolution rate. This effect was successfully modeled by combining a dissolution model with a grinding model (size–mass balance) from the milling literature. This model establishes a basis for predicting the dissolution rate of solids in an agitated slurry such as a soil–slurry bioreactor.

Model Development

Dissolution only

The dissolution of TNT solids into aqueous solution (batch, stirred-tank system) was modeled with the following equation

$$\frac{dC}{dt} = k_L a(C^* - C), \tag{1}$$

where
k_L = solid–liquid mass-transfer coefficient (m/s)
a = TNT particle surface-area/solution volume (m^2/m^3)
C = TNT concentration in bulk solution (kg/m^3)
C^* = equilibrium TNT concentration at solid–liquid interface (kg/m^3)

A number of correlations for k_L in stirred-tank systems have been reported in the literature (Armenante and Kirwan, 1989; Levins and Glastonbury, 1972b; Calderbank and Moo-Young, 1961; Nienow, 1992). The similarity of these correlations as well as the inaccuracy of reported experimental values makes it difficult to recommend one correlation over the others (Nienow, 1992). For this work, the correlation of Levins and Glastonbury (1972b) was used

$$Sh = \frac{k_L d_p}{D_w} = 2 + 0.47 Re_p^{0.62} Sc^{0.36} \left(\frac{d_S}{d_T}\right)^{0.17}, \tag{2}$$

where
d_p = TNT particle diameter (m)
d_S, d_T = stirrer, tank diameter (m)
D_w = diffusivity of TNT in water (m^2/s)
Re_p = particle Reynolds number
Sc = Schmidt number = ν/D_w
Sh = Sherwood number
ν = kinematic viscosity (m^2/s)

For D_w at 30°C, a value of 0.57×10^{-5} cm^2/s was regressed from dissolution rate data (see Figure 2, in Results and Discussion).

If agitation conditions are characterized in terms of the power input per unit mass of slurry (ϵ), then the particle Reynolds number can be defined as (Levins and Glastonbury, 1972b)

$$Re_p = \frac{\epsilon^{1/3} d_p^{4/3}}{\nu}. \tag{3}$$

Equation 3 can also be derived from Kolmogoroff's theory of local isotropic turbulence (Levins and Glastonbury, 1972a). Questions have been raised as to the applicability of this definition, since it implies that k_L is a unique function of ϵ, independent of reactor geometry. Some experiments have shown that different agitators give very different k_L values at equal ϵ (Nienow, 1992). Nonetheless, the Kolmogoroff definition for Re_p is widely used, and it provided reasonable results for our experimental system.

Slurry effects on the solid–liquid mass-transfer coefficient

A method described by Kikuchi et al. (1987b) was used to predict k_L in a PTFE chip slurry. Equation 2 was still used to determine k_L, but the particle Reynolds number (Re_p) was modified as shown in Eq. 4 to account for the increased kinematic viscosity of the slurry

$$Re_p = \frac{\epsilon_m^{1/3} d_p^{4/3}}{\nu_m} \tag{4}$$

where
ϵ_m = power per unit mass of water, not total mass (m^2/s^3)
$\nu_m = \mu_m/\rho_m$ = kinematic viscosity of slurry (m^2/s)

The components of the kinematic viscosity, μ_m and ρ_m, are calculated using Eqs. 5 and 6, respectively

$$\mu_m = \mu_w \left[1 - \left(\frac{\alpha}{\alpha_{\max}}\right)\right]^{-2.5\alpha_{\max}}, \tag{5}$$

where
α = volume fraction of PTFE in the slurry
$\alpha_{\max}$ = maximum volume fraction of PTFE (bulk density for a packed column of PTFE chips divided by the true density of PTFE)
μ_w = viscosity of water (kg/m/s)

$$\rho_m = (1 - \alpha)\rho_w + \alpha\rho_p \tag{6}$$

where
ρ_w = density of water (kg/m^3)
ρ_p = density of PTFE (kg/m^3)

The Schmidt number in the Levins and Glastonbury correlation (Eq. 2) was defined using the kinematic viscosity of water.

Size–mass balance for grinding without dissolution

When TNT beads were added to an agitated PTFE slurry, breakage/attrition of the TNT solids resulted. Thus, a model for TNT dissolution in this system must account for changes in the TNT particle-size distribution (PSD) with time due to grinding. The *size–mass balance* has been successfully used

to model the time-variant PSDs in batch ball mill systems. Austin and coworkers (1984) have written a thorough treatise on this subject, and the following grinding model was adopted from their text.

For experiments in which no TNT dissolution occurred (grinding only), the size–mass balance was

$$\frac{dW_i(t)}{dt} = -S_i W_i(t) + \sum_{j=1}^{i-1} b_{i,j} S_j W_j(t), \tag{7}$$

where $W_i(t)$ is the total mass of size i particles (TNT) in the reactor at time t. The size–mass balance consisted of 15 size intervals corresponding to a standard ($\sqrt{2}$) geometric screen series. Size intervals were numbered from $i=1$ (feed or largest interval) to n (sink or smallest interval), where i refers to the upper size limit of an interval. The first term on the right side of Eq. 7 represents the loss of size i material due to grinding; a breakage rate that is first order with respect to $W_i(t)$ was assumed. Here, S_i is the specific rate of breakage for the ith size interval; Eq. 8 was used to describe S_i as a function of size (x_i)

$$S_i = \sigma \left(\frac{x_i}{1{,}000\ \mu\text{m}} \right)^{\omega} \left(\frac{1}{1 + (x_i/\tau)^{\Lambda}} \right), \tag{8}$$

where x_i is the upper limit of the ith size interval (μm). As typically observed in grinding experiments, S_i increases with particle size (x_i) to a maximum at size x_m; S_i then decreases for sizes larger than x_m. The fitting parameters σ, ω, τ, and Λ were derived from TNT grinding experiments.

The quantity $b_{i,j}$ in Eq. 7 is defined as the *progeny fragment distribution*, which represents the fraction of material broken from size j that appears in the smaller size interval i ($i > j$). Thus, the second term on the right side of Eq. 7 represents the fraction of breakage from a larger size interval j that produces smaller size i particles. Progeny fragment distributions are normally plotted in the cumulative form, in which $B_{i,j}$ is the cumulative weight fraction of material broken from size j that appears as particles smaller than the upper size of interval i ($b_{i,j} = B_{i,j} - B_{i+1,j}$). For the TNT grinding model used in this study, $B_{i,j}$ was represented by Eq. 9

$$B_{i,j} = \phi \left(\frac{x_{i-1}}{x_j} \right)^{\gamma} + (1-\phi) \left(\frac{x_{i-1}}{x_j} \right)^{\beta}. \tag{9}$$

This equation assumes that all of the PSDs are dimensionally similar or *normalized*; it is often appropriate for PSDs associated with *normal breakage* (observed when a significant number of impacts result in particle fracture) (Austin et al., 1984). The fitting parameters ϕ, γ, and β also were derived from TNT grinding experiments.

Size – mass balance for simultaneous grinding and dissolution

To account for the combined effects of particle breakage and dissolution, three dissolution terms were added to the size–mass balance shown in Eq. 7. The first term accounts for the loss of material in size interval i due to dissolution. This may be expressed as

$$\frac{dW_i(t)}{dt} = -k_i A_i (C^* - C), \tag{10}$$

where A_i is the total TNT particle surface area for size fraction i (m^2) and k_i is the value of k_L for particles in this size fraction (m/s). The diameter used in calculating A_i and k_i was the median value for size fraction i.

The second and third additional terms account for particles that dissolve out of and into size fraction i. In this case, particle-size reduction is due to dissolution rather than grinding. If it is assumed that the size distribution within interval i is flat, the weight fraction of particles reduced to the next size fraction is equivalent to $d(d_p)/\Delta X_i$. In this ratio, $d(d_p)$ is the differential reduction in particle size due to dissolution, and ΔX_i is the width of size interval i (m). Thus, we can write:

$$\frac{dW_i(t)}{dt} = \left(\frac{d(d_p)}{dt} \right) \left(\frac{W_i(t)}{\Delta X_i} \right). \tag{11}$$

However, since the rate of change in diameter of a spherical particle due to dissolution is given by

$$\frac{d(d_p)}{dt} = \frac{-2k_L}{\rho_T} (C^* - C), \tag{12}$$

where ρ_T is the density of the particle (kg/m^3), and Eq. 11 can be written in the form

$$\frac{dW_i(t)}{dt} = \frac{-2k_i}{\rho_T \Delta X_i} (C^* - C) W_i(t). \tag{13}$$

A similar equation written for size fraction $i-1$ would account for the particles that enter size fraction i by dissolution. Addition of these dissolution terms to Eq. 7 (with appropriate attention to signs), yields

$$\frac{dW_i(t)}{dt} = \sum_{j=1}^{i-1} b_{i,j} S_j W_j(t) - S_i W_i(t) - k_i A_i (C^* - C) - \frac{2k_i}{\rho_T \Delta X_i} (C^* - C) W_i(t) + \frac{2k_{i-1}}{\rho_T \Delta X_{i-1}} (C^* - C) W_{i-1}(t). \tag{14}$$

Terms 1 and 5 on the right side of Eq. 14 disappear for $i=1$ (top size interval), and terms 2 and 4 disappear for $i=n$ (sink interval). To model TNT dissolution with grinding, the n equations for $dW_i(t)/dt$ were integrated simultaneously with the following equation for aqueous TNT concentration

$$\frac{dC}{dt} = \sum_{i=1}^{n} k_i a_i (C^* - C), \tag{15}$$

where a_i is the TNT particle surface area per unit solution volume for particles in the ith size interval [m^2/m^3]. Once again, k_i and a_i were based on the median diameter of the size interval.

Materials and Methods

Vessel setup

An Applikon 3.0-L stirred vessel with three baffles and a dished bottom was used in all experiments. A 60-mm vortexing marine impeller (Applikon model Z81314RC07) was used for agitation. The center of this impeller was 3.8 cm above the bottom of the vessel. The total working volume (PTFE and water) was 2.0 L.

Indicated torque and rpm readings from an Applikon P100 motor controller were used to determine agitator power input. Indicated agitator speed was verified with an Ametek Model 1723 RPM meter. Indicated torque readings were calibrated by Magtrol, Inc., using a dynamometer. Bearing losses were estimated by running the motor attached to the empty vessel without an impeller on the shaft. These losses were substracted from the indicated power for each experiment.

Spherical TNT bead fabrication

For the dissolution experiments, spherical TNT particles of known diameter were needed so that a reasonable estimate of the surface area for dissolution could be made. While spherical particles (beads) were not required or completely realistic for the grinding experiments, it was necessary to start with TNT particles from a single sieve size fraction. The same procedure for creating spherical particles for dissolution experiments also provided a safe, efficient means of creating same-sized particles for grinding experiments.

TNT beads were fabricated by melting TNT flakes (Chem Service, Inc., 99.0% purity) in hot water (>80°C) and agitating the molten TNT/hot water solution to create TNT droplets. The droplet suspension was then quickly transferred to a flask filled with ice water to freeze the TNT in spherical form. To remove abnormally weak edges from particles, the TNT beads were agitated in the vessel with saturated aqueous TNT solution (500 rpm for 30 min, no PTFE). The TNT beads were then classified into size fractions by wet sieving. Particles that would not easily roll off a PTFE-coated pan or appeared nonspherical to the naked eye were removed by hand. Due to the explosive nature of TNT, particles were handled wet whenever possible; extreme care was taken to avoid any explosure of TNT to heat or shock. Figure 1 is a photograph of the TNT beads fabricated for these experiments.

PTFE chips

PTFE boiling chips (Norton), 4–8 mesh (2.36–4.75 mm) in size were used in all the slurry experiments; this material was chosen because it does not sorb TNT from aqueous solution (Gilcrease, 1997). Prior to each grinding experiment, the PTFE chips were washed with an Alconox solution and rinsed with filtered, deionized water to remove any dirt or residual TNT.

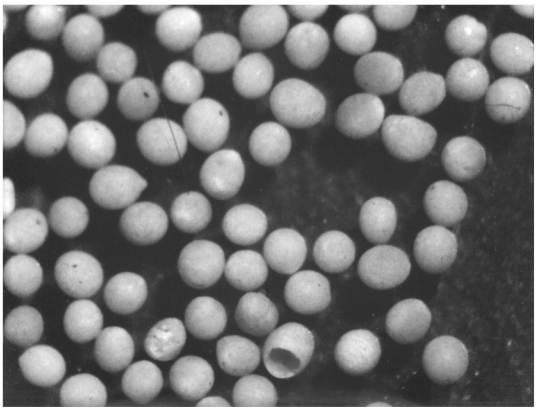

Figure 1. Appearance of spherical TNT beads (600–710 μm) prior to dissolution/grinding experiments.

TNT dissolution experiments

Spherical TNT beads 600–710 μm in initial size were used for the dissolution experiments. The initial charge of TNT beads varied between 0.4002 and 0.4011 g. The TNT beads were agitated at 30°C in either deionized water or a PTFE/water slurry, and the concentration of TNT in solution was monitored via HPLC. Aqueous HPLC samples were filtered (1.0-μm fiberglass) to remove any TNT fines, then diluted with an equal volume of acetonitrile. The isocratic HPLC method used a Rainin Microsorb C8 80-315-C5 column and a mobile phase consisting of 50% sulfuric acid (0.003 N) solution and 50% acetonitrile. The total flow rate was held constant at 1.0 mL/min. TNT was quantified by measuring A_{254} with a Waters 486 tunable absorbance detector. TNT standards were obtained from Supelco, Inc.

Slurry k_L values via ion-exchange experiments

Slurry k_L values in PTFE slurries were measured using cation-exchange resin, as described by Levins and Glastonbury (1972b). Dowex 50W-X8 (Dow Chemical), a strongly acidic cation-exchange resin, was allowed to swell in distilled water before a 600–710-μm-size fraction was collected via wet sieving. Before each experiment, the resin was regenerated to the hydrogen form with 1.0 N sulfuric acid. At time zero, a known volume of resin (~ 8 mL) was added to the 30°C reactor containing 5×10^{-4} M NaOH and 0–30 vol. % PTFE chips (vol. % values represent the chip volume as a percent of the total slurry volume). The neutralization ($Na^+ - H^+$ exchange) was followed on-line with a YSI 3417 conductivity probe connected to a YSI Model 35 Conductance Meter. The conductivities of known NaOH standards at 30°C were used to convert conductivity to concentration.

Two difficulties are associated with using ion-exchange particles to measure liquid-side mass-transfer coefficients (k_L). First, it must be established that the ion-exchange process is controlled by interparticle (film) diffusion rather than intraparticle diffusion. Experiments and calculations were used to verify that the exchange was film-diffusion limited for

these conditions (Gilcrease, 1997). The second difficulty is choosing an appropriate value for the effective diffusivity (D_{eff}) when correlating the mass-transfer coefficient k_L (Kikuchi et al., 1987a). Since the Levins and Glastonbury correlation (Eq. 2) provided reasonable k_L values for TNT dissolution in our vessel (Results and Discussion), D_{eff} was chosen such that the k_L value observed for ion-exchange experiments at 0% PTFE, 800 rpm, and 30°C would match the value predicted by Eq. 2 ($D_{\text{eff}} = 3.02 \times 10^{-5}$ cm^2/s). This value lies between the self-diffusivities of Na^+ and H^+ in water at infinite dilution, as expected (Gilcrease, 1997).

TNT grinding experiments

Approximately 0.5 g of dry TNT beads, 600–710 μm in size initially, was added to the stirred vessel containing filtered (0.45 μm nylon), saturated (125 mg TNT/L) solution and clean PTFE chips. At time zero, agitation of the reactor (800 rpm) was started. Experiments were run at room temperature (approximately 25°C, with a variation of ± 0.5°C during the experiment). Duplicate HPLC samples were taken before and after each experiment; before dilution with acetonitrile, samples were filtered (1.0-μm fiberglass). The presence of suspended TNT particles less than 1.0 μm in diameter was indicated when the filtered sample concentration was higher than the aqueous saturation concentration.

TNT particle collection

After the specified agitation time, PTFE chips were collected on a 1.18-mm sieve, and the TNT particles on a 1.0-μm polycarbonate filter (Nucleopore). Smaller TNT particles tended to stick to the PTFE chips, which had to be washed to improve TNT material balances. Unwashed PTFE was placed on the 1.18-mm sieve in amounts just sufficient to cover the sieve surface, and filtered, saturated TNT solution was used to wash TNT fines from the PTFE chips. Collected TNT particles were dried overnight at approximately 15 in. Hg vacuum and 45°C. The collected TNT was weighed for material balance purposes prior to particle-size analysis.

Particle-size analysis

TNT particle-size analysis was performed by Particle Technology Labs, Ltd. Particles greater than 250 μm were quantified via sieve analysis, and those less than 250 μm were analyzed using an Elzone particle-size analyzer (Coulter Counter technique). Results for the two analytical methods were combined for each sample to obtain the complete particle-size distribution. TNT solids recoveries varied between 69 and 100%, declining with increased grinding times and fines production. An estimated particle-size distribution for missing fines was used to correct PSDs where the recovery was less than 100% (Gilcrease, 1997).

Numerical methods

Parameters for Eqs. 8 and 9 were backcalculated from experimental grinding data using the MILLLEN1 program written by Dr. L. G. Austin (The Pennsylvania State University). This program uses a proprietary optimization routine developed by Dr. T. J. Trimarchi (The Pennsylvania State University) to determine best-fit parameters. Best-fit grinding parameters for a particular milling condition (rpm and vol. % PTFE) were regressed from several grinding experiments run at that same condition but at different batch times.

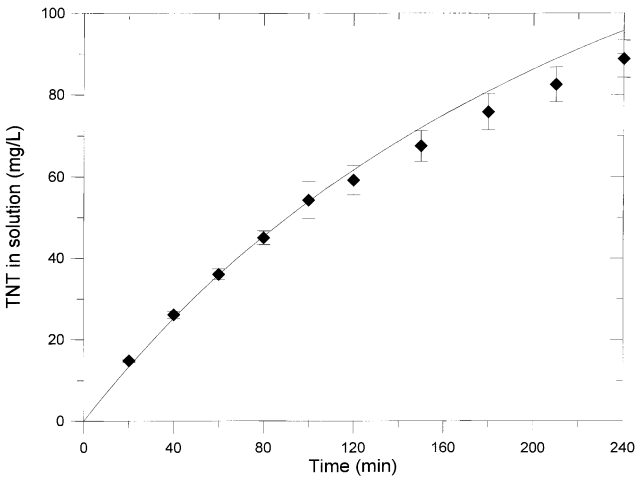

Figure 2. Dissolution of TNT beads without PTFE at 500 rpm.

Observed concentrations (symbols) and DISSLURR program prediction (curve).

For the dissolution-only model, Eq. 1 was integrated using the Levins and Glastonbury correlation (Eq. 2) to determine k_L values. The program DISSLURR solves the dissolution-only model using POLYMATH (Shacham and Cutlip, 1994). DISSLURR accounts for reductions in particle diameter due to dissolution, but it does not include any grinding effects. For PTFE slurry systems, DISSLURR accounts for slurry viscosity effects on k_L via Eq. 4.

Programs to solve the grinding (size–mass balance) models were written in Fortran and used a fourth-order Runge-Kutta algorithm for simultaneous numerical integration (Gilcrease, 1997). In the grinding-only program (GRIND), Eq. 7 was integrated for 15 size fractions ($\sqrt{2}$ standard sieve series). In the grinding-with-dissolution program (GRINDIS), Eqs. 14 (15 size intervals) and 15 were integrated simultaneously.

Results and Discussion

Dissolution of TNT solids (no PTFE slurry)

These experiments were used to test the validity of Eq. 2 for prediction of TNT dissolution in our stirred vessel. Levins and Glastonbury (1972b) reported that the standard deviation of 357 experimental points from the line of best fit (Eq. 2) was 8.3%. Figure 2 shows our experimental data for the dissolution of 0.400-g TNT beads (600–710 μm in diameter) at 30°C and 500 rpm. The TNT particles were completely suspended under these conditions. Symbols denote average TNT concentrations for triplicate experiments ± 1 standard deviation. Conformity between the DISSLURR model (solid line in Figure 2) and experiment was quite good, with an r^2 value of 0.983. Similar agreement between model and experiment was observed for a range of TNT particle sizes and agitator speeds (Gilcrease, 1997). These results indicated that Eq. 2 was valid for our system; thus, it was used throughout the study to predict solid–liquid k_L values.

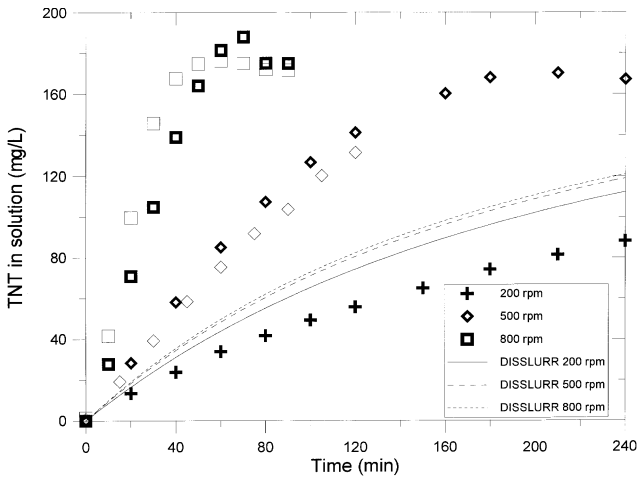

Figure 3. Dissolution of TNT beads in a 29 vol. % PTFE slurry.

Observed concentrations (symbols) and DISSLURR program predictions (curves).

Dissolution of TNT solids in a PTFE slurry

Preliminary experiments for determining the PTFE slurry effect on k_L were conducted with dissolving TNT beads. Figure 3 shows TNT dissolution data for 29 vol. % PTFE slurries at 200, 500, and 800 rpm; thin symbols denote duplicate experiments at 500 rpm and 800 rpm. PTFE chips were not suspended at 200 or 500 rpm, but they were near the suspension point at 800 rpm. Dissolution curves as predicted by DISSLURR are also shown; Re_p was defined as in Eq. 4 to account for slurry kinematic viscosity effects. At 200 rpm, dissolution was slightly slower than predicted; it will be shown that the Kikuchi method (using Eq. 4) underpredicts k_L values when the slurry is not suspended. However, at 500 and 800 rpm the observed dissolution rates were much faster than predicted. Undissolved TNT particles were collected and examined at the end of each experiment; particle breakage was visibly apparent at 500 and 800 rpm, but not at 200 rpm. Two important conclusions were drawn from these preliminary experiments: (1) TNT beads could not be used to isolate the effect of PTFE slurry concentration on k_L because the surface area of the broken particles was unknown; (2) the anticipated negative effect of slurry kinematic viscosity on k_L was overshadowed by an increase in surface area due to particle breakage.

Slurry effect on k_L (ion-exchange experiments)

To isolate the effect of solids concentration on k_L at constant agitator speeds, mass-transfer experiments were conducted in PTFE slurries with ion-exchange particles. These particles were not damaged when agitated in PTFE slurries, and thus provided a known constant surface area for mass transfer. Experimental k_L values for PTFE slurries are compared with values predicted by the Kikuchi method in Figure 4. At 800 rpm, the experimental k_L values were within 6% of the predicted values for 0 through 30 vol. % PTFE. At this stirrer speed, the 20 vol. % slurry was suspended, and the 30 vol. % slurry was close to the suspension point. As predicted, k_L decreased 26% as the vol. % PTFE was increased from 0% to 30%. At the higher PTFE concentrations, turbulence levels were damped (due to the higher effective viscosity of the slurry), resulting in lower k_L values for the same agitator speed.

It was not clear from Kikuchi et al. (1987b) whether the Schmidt number should be defined using the aqueous (ν) or slurry (ν_m) kinematic viscosity. Using ν_m to define Sc resulted in overprediction of the k_L values and only a slight drop (2%) over the range from 0% to 30% PTFE at 800 rpm. Therefore, Sc was defined in terms of water properties; this may reflect the fact that the viscosity of the boundary-layer fluid (water) is not affected by the slurry concentration. While the bulk viscosity of the system *is* influenced by the slurry concentration, the viscosity of the fluid immediately surrounding the TNT particle does not change.

Predicted and observed k_L values at 500 rpm for 0 to 20 vol. % PTFE are also shown in Figure 4. In this case, a 29% decrease in k_L was observed when the slurry concentration was increased from 0 vol. % to 20 vol. % PTFE. This compares with a predicted decrease of only 3.8%. For 20 vol. % PTFE, the observed k_L values were 15 to 22% lower than predicted. At this loading, the PTFE chips were not in suspension; thus, the correlation may overpredict k_L values when the slurry is not suspended. For the remaining 500 rpm data points, the slurry was either suspended (10 vol. %) or not present (0 vol. %), and the observed k_L values were within 11% of the predicted values. Kikuchi et al. (1987b) also report a satisfactory agreement between experimental and predicted Sh values when Eq. 4 was used to define Re_p; the particles were completely suspended in these experiments. They used glass or polystyrene beads as inert slurry particles, and their slurry concentrations ranged from 0 vol. % to 50 vol. %. Overall, these results indicate that the Kikuchi method provides reasonable k_L values for agitated PTFE slurries (not accounting for particle breakage, and provided the slurry is near the suspension point). Thus, it was used to account for the effect of slurry viscosity on k_L in all slurry system models (DISSLURR and GRINDIS).

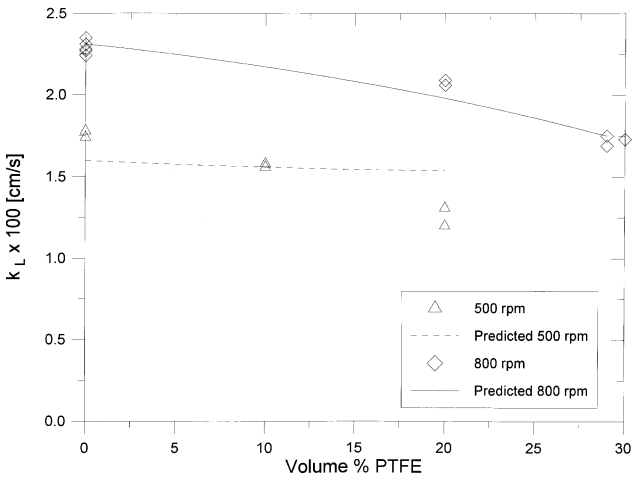

Figure 4. Effect of PTFE slurry concentration on ion-exchange particle k_L values.

Symbols denote observed values. Predicted curves are from Eq. 2 using Eq. 4 for Re_p.

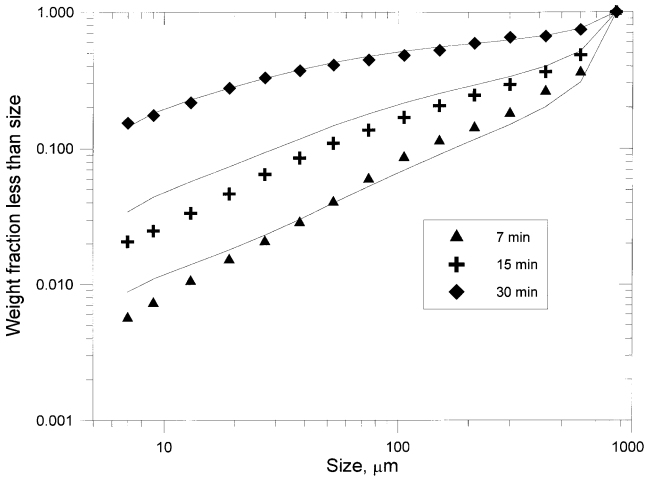

Figure 5. TNT particle-size distributions after grinding in a 29 vol. % PTFE slurry at 800 rpm.

Observed values (symbols) and GRIND program predictions (curves).

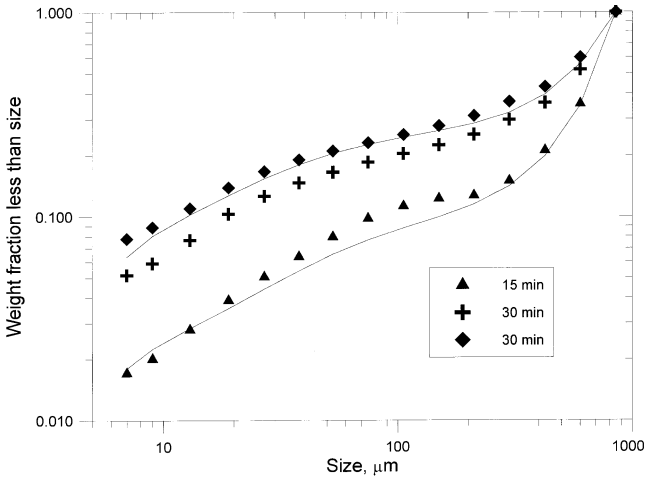

Figure 6. TNT particle-size distributions after grinding in a 15 vol. % PTFE slurry at 800 rpm.

Observed values (symbols) and GRIND program predictions (curves).

Grinding of TNT in a PTFE slurry (no dissolution)

To account for grinding effects on TNT surface area and dissolution rates, TNT grinding experiments were conducted in agitated PTFE slurries. Conditions were identical to the 800 rpm experiments in Figure 3, except that the aqueous phase was presaturated with TNT. This eliminated any dissolution effects; thus, the observed changes in TNT PSDs were the result of grinding effects only. PSDs from grinding-only experiments were used to determine best-fit values for the parameters in Eqs. 8 and 9 (GRIND program) for both 15 and 29 vol. % PTFE slurries. These same parameters were then used in the grinding with dissolution model (GRINDIS program) to predict TNT dissolution in PTFE slurries (see below).

Experimental PSD curves for a 29 vol. % PTFE slurry agitated at 800 rpm are shown in Figure 5 for 7-, 15- and 30-min grinding times. These curves are presented in *cumulative* form, in which each point represents the weight fraction of TNT particles less than the indicated size. Predicted curves are also shown for each grinding time; these curves were generated with the GRIND program using best-fit parameters from the MILLLEN1 program. Best-fit grinding parameters for each condition are listed in Table 1. The fit between *interval* data and model predictions was assessed using an r^2 calculation based on sum of squares. The r^2 values were 0.990, 0.994, and 0.920 for the 7-, 15- and 30-min curves, respectively, indicating a good description of the data by the model.

Table 1. Best-Fit TNT Grinding Parameter Values from the MILLLEN1 Program*

Grinding Parameter	29 vol. % PTFE	15 vol. % PTFE
S_i Parameters		
σ (min^{-1})	0.509	2.284
ω	0.406	0.846
τ (mm)	0.4	0.2
Λ	3	3
$\dot{B}_{i,j}$ Parameters		
ϕ	0.085	0.184
γ	0.425	0.547
β	2	4.471

*Equation 8 was used to model S_i, and Eq. 9 was used to model the $B_{i,j}$ distributions.

Figure 6 shows PSD curves for a 15 vol. % PTFE slurry at 800 rpm for 15- and 30-min grind times. Two experiments were run at 30 min to determine reproducibility. Best-fit grinding parameters for the three runs are shown in Table 1. The model fits the 30-min data well ($r^2 = 0.997$), but the match to the plateau region (100–250 μm) of the 15-min data was less satisfactory. The plateau in the 15-min data suggests that particle attrition was more prevalent for these conditions (as opposed to normal breakage). The form of the $B_{i,j}$ correlation (Eq. 9) used in the model is meant to fit progeny fragment distributions resulting from normal breakage rather than attrition. Still, the correlation coefficient for the interval data at 15 min was quite good ($r^2 = 0.999$). Given the uncertainty of the PSD data associated with lower collection efficiencies, the GRIND program provides an adequate means of accounting for changes in TNT PSDs due to grinding in our system.

Grinding and dissolution of TNT in a PTFE slurry

At this point, separate expressions for the effects of PTFE particles on k_L and the PSD had been developed and validated. The next step was to incorporate dissolution expressions into the size–mass balance to model the simultaneous grinding and dissolution of TNT particles in PTFE slurries (GRINDIS program). In Figure 7, the 800-rpm data from Figure 3 are compared with the GRINDIS generated curve that accounts for slurry viscosity and particle breakage. Symbols show average values for the two runs ± 1 standard deviation. Grinding parameters for GRINDIS (Table 1, 29 vol. PTFE) were derived from the grinding-only experiments shown in Figure 5, which were conducted at the same agitator speed and PTFE concentration. While the GRINDIS-

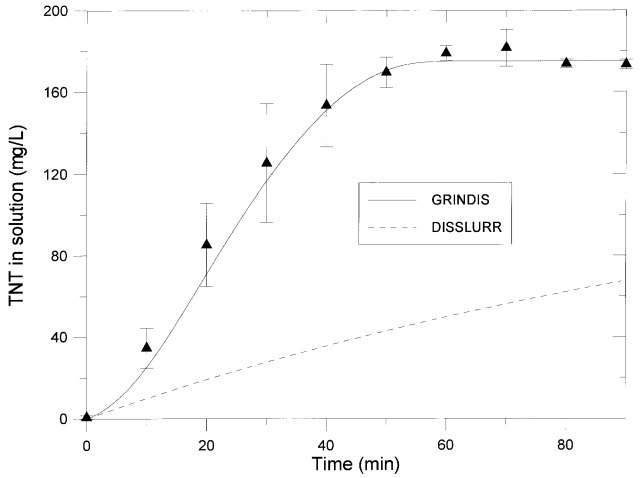

Figure 7. Dissolution of TNT beads in a 29 vol. % PTFE slurry at 800 rpm.

Observed concentrations (symbols) are compared with GRINDIS and DISSLURR program predictions (curves).

predicted curve was slightly lower than the average data points (27% at 10 min, 2% at 40 min), this was a marked improvement over the dissolution-only model (DISSLURR). The r^2 value for the GRINDIS curve was 0.989. Comparison of the experimental curve with that predicted by the dissolution-only model again illustrates the enhanced dissolution due to particle breakage: after 60 min, the GRINDIS estimated ($k_L a$) value was 118 times the value predicted by DISSLURR.

Results for TNT dissolution in a 15 vol. % PTFE slurry at 800 rpm are shown in Figure 8. In this case, the observed dissolution rate was not as high as for 800 rpm, 29 vol. % PTFE; the estimated ($k_L a$) value after 10 min was 2.1×10^{-4} s^{-1}, compared with 4.3×10^{-4} s^{-1} for 29 vol. % PTFE. This was in agreement with the lower breakage rate observed in the grinding-only experiments for these conditions (Gilcrease, 1997). Agreement between the GRINDIS curve and experiment was excellent, as indicated by the $r^2 = 0.999$ value. Grinding parameters were derived from the 800-rpm, 15 vol. % PTFE milling data shown in Figure 6 (see Table 1, 15 vol. % PTFE for parameter values). The estimated GRINDIS ($k_L a$) value at 60 min was 9.1 times that estimated with the dissolution-only model.

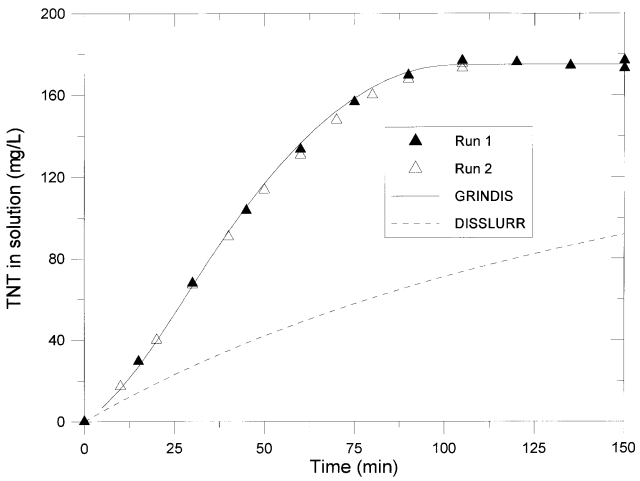

Figure 8. Dissolution of TNT beads in a 15 vol. % PTFE slurry at 800 rpm.

Observed concentrations (symbols) are compared with GRINDIS and DISSLURR program predictions (curves).

Significance of work

The most basic model for solids dissolution (Eqs. 1 and 2) does not account for slurry viscosity effects on k_L, and assumes that the surface area for dissolution (a) is constant with respect to time. The effect of slurry viscosity (turbulence damping) on k_L was accounted for using the Kikuchi method (Eqs. 4–6), but this model does not account for surface area changes associated with grinding. Because grinding has a significant, positive effect on dissolution rates in our system (Figure 3), a knowledge of the changing TNT solids PSD was needed to accurately account for a as a function of time. This was accomplished via a size–mass balance, but Eq. 7 is only valid for mechanical grinding without dissolution. Our expanded size–mass balance (Eq. 14) is novel because it includes the effects of dissolution on the PSD. When integrated simultaneously with the dissolution model (Eq. 15), this new size–mass balance predicts dissolution rates when grinding is present. The effect of PSD on k_L is accounted for by calculating separate k_L values for each size fraction (k_i), where each k_i is corrected for slurry viscosity effects. Our final combined model (GRINDIS) simultaneously accounts for all the observed slurry effects on $k_L a$ (damping and grinding with dissolution), while the three previous models omit one or more of these effects.

Potential applications

While solid dissolution rates are often enhanced via dry milling of the material prior to dissolution in an agitated vessel, the explosive nature of dry TNT prohibits using a separate pregrinding step. The aqueous slurry process presented here provides a safe means of wet grinding TNT solids to promote simultaneous dissolution. In the biodegradation of TNT solids, dissolution can be the rate-limiting step, since TNT in aqueous solution is more readily available to the degrading microorganisms (Gilcrease et al., 1996; Gilcrease, 1997). We anticipate that a similar grinding effect will be observed when soil slurries contaminated with TNT solids are agitated. In this case the soil particles act as the grinding medium, and agitation can significantly enhance the overall biodegradation rate. The rate/extent of TNT grinding will be dependent on the soil type and size; thus, grinding experiments in real soil slurries are needed to obtain the appropriate grinding model parameters.

The model developed in this study could readily be used to predict dissolution rates for any system where milling and dissolution of solids occurs simultaneously. Combining these two unit operations might be advantageous in a number of situations: (1) dissolving oxygen-sensitive materials that might oxidize during dry milling; (2) studies have shown that breakage rates for wet grinding may be 1.1 to 2.0 times those for dry grinding, leading to overall mill capacity increases of 30% at the industrial scale (Austin et al., 1984); (3) finer material

produced during milling can dampen collisions inside a mill, resulting in lower breakage rates for the remaining coarse material (Austin et al., 1984); thus, simultaneous dissolution would effectively remove these finer particles and increase mill efficiency; (4) by conducting the dissolution step inside the mill, a separate stirred tank for dissolution could be eliminated (along with an additional solids-handling step), reducing the overall process capital costs.

One system amenable to simultaneous grinding and dissolution is the chemical/biological leaching of sulfide minerals such as sphalerite (ZnS), chalcopyrite ($CuFeS_2$), and pyrite (FeS_2). The leaching of sphalerite and chalcopyrite provides a means of recovering zinc and copper, respectively. Pyrite is often associated with other sulfidic ore materials (containing copper, nickel, zinc, uranium, or gold), and must be leached prior to recovery of the desired mineral (Tuovinen, 1990). Pyrite can also be leached from coal to reduce sulfur dioxide emissions during combustion. During the leaching of sulfide minerals, sulfur or jarosite precipitate layers may form on the surface, limiting the leach rate (Boon and Heijnen, 1993; Rice et al., 1991). Rice et al. (1991) suggested that grinding during the leaching process can prevent such layers from forming. While various kinetic models have been proposed for sulfide leaching, in each case the rate is proportional to the exposed surface area (Boon and Heijnen, 1993); thus, changes in the mineral surface area with grinding would need to be accounted for in the rate expression. Another application involves the reaction of niobium solids with hexane or methanol during mechanical grinding (Kaneyoshi et al., 1993); again, the change in reactive surface area due to grinding must be accounted for. Validation of the grinding with dissolution model (GRINDIS) in this study suggests a general approach to modeling fluid–solid reactions when the particle surface area is changing due to comminution, that is, coupling the fundamental rate equation with a size–mass balance.

Finally, it should be noted that GRINDIS could be used to model a crystallization process in which formation and growth of breakage/attrition fragments is the predominant mechanism. By altering the subscripts on terms 4 (i to $i+1$) and 5 ($i-1$ to i), Eq. 14 can account for mass-transfer-limited fragment growth when C is greater than C^*. Such a crystallization model may not be realistic; attrition or fracture pieces grow at a lower rate, and are typically not significant nucleation sources compared to contact nucleation (Randolph and Larson, 1988). Equation 14 as written would not account for growth of nuclei produced by contact nucleation. However, Gahn and Mersmann (1999) state that attrition can be a dominant source of growth nuclei when the product crystal size is large; they propose a similar modeling approach (population balance combined with crystal-growth kinetics) for this type of crystallizer.

Conclusions

Two separate effects of solids loading on solid–liquid mass transfer were observed in this study: (1) a decrease in k_L associated with turbulence damping, and (2) an increase in a due to slurry grinding effects. For the dissolution of TNT particles, the overall mass-transfer rate increased considerably with PTFE loading at constant rpm levels. This indicates that slurry grinding can be an important mechanism for enhancing the dissolution of solids such as TNT. This study is also significant because it successfully combines three previously developed models to account for solids dissolution in an agitated slurry. The negative effect of PTFE solids on k_L values was reasonably predicted with an equation that accounts for turbulence damping due to slurry viscosity. The size–mass balance, when combined with a classic dissolution expression and the slurry viscosity correction, proved to be an excellent tool for modeling and predicting the positive effect of slurry grinding on solids dissolution rates.

Acknowledgments

This work was supported by the J. R. Simplot Company and the Colorado Institute for Research in Biotechnology.

We thank Dr. L. G. Austin, The Pennsylvania State University, for technical advice on milling experiments and the grinding model.

Literature Cited

Armenante, P. M., and D. J. Kirwan, "Mass Transfer to Microparticles in Agitated Systems," *Chem. Eng. Sci.*, **44**, 2781 (1989).

Austin, L. G., R. R. Klimpel, and P. T. Luckie, *Process Engineering of Size Reduction: Ball Milling*, Society of Mining Engineers, New York (1984).

Boon, M., and J. J. Heijnen, "Mechanisms and Rate Limiting Steps in Bioleaching of Sphalerite, Chalcopyrite, and Pyrite with *Thiobacillus ferrooxidans*," *Biohydrometallurgical Technologies*, A. E. Torma, J. E. Wey, and V. L. Lakshmanan, eds., Minerals, Metals and Materials Soc., p. 217 (1993).

Calderbank, P. H., and M. B. Moo-Young, "The Continuous Phase Heat and Mass-Transfer Properties of Dispersions," *Chem. Eng. Sci.*, **16**, 39 (1961).

Conti, R., and A. W. Nienow, "Particle Abrasion at High Solids Concentration in Stirred Vessels: II," *Chem. Eng. Sci.*, **35**, 543 (1980).

Gahn, C., and A. Mersmann, "Brittle Fracture in Crystallization Processes Part B. Growth of Fragments and Scale-Up of Suspension Crystallizers," *Chem. Eng. Sci.*, **54**, 1283 (1999).

Gilcrease, P. C., V. G. Murphy, and K. F. Reardon, "Bioremediation of Solid TNT Particles in a Soil Slurry Reactor: Mass Transfer Considerations," *Proc. HSRC/WERC Joint Conf. on the Environment*, L. E. Erickson, D. L. Tillison, S. C. Grant, and J. P. McDonald, eds., Great Plains/Rocky Mountain Hazardous Substance Research Center, Manhattan, KS, 152 (1996).

Gilcrease, P. C., "Mass Transfer Effects on the Bioreduction of TNT Solids in Slurry Reactors," PhD Diss., Colorado State Univ., Fort Collins (1997).

Ishii, M., and N. Zuber, "Drag Coefficient and Relative Velocity in Bubbly, Droplet or Particulate Flows," *AIChE J.*, **25**, 843 (1979).

Kaneyoshi, T., T. Takahashi, and M. Motoyama, "Reaction of Niobium with Hexane and Methanol by Mechanical Grinding," *Scr. Met. Mater.*, **29**, 1547 (1993).

Kikuchi, K.-I., M. Niyama, T. Sugawara, and H. Ohashi, "Estimation of Diffusivity for Correlation of Mass Transfer Coefficient Between Particles and Liquid in Ion Exchange in a Stirred Tank," *J. Chem. Eng. Jpn.*, **20**, 421 (1987a).

Kikuchi, K.-I., Y. Tadakuma, T. Sugawara, and H. Ohashi, "Effect of Inert Particle Concentration on Mass Transfer Between Particles and Liquid in Solid-Liquid Two-Phase Upflow Through Vertical Tubes and in Stirred Tanks," *J. Chem. Eng. Jpn.*, **20**, 134 (1987b).

Levins, D. M., and J. R. Glastonbury, "Application of Kolmogoroff's Theory to Particle-Liquid Mass Transfer in Agitated Vessels," *Chem. Eng. Sci.*, **27**, 537 (1972a).

Levins, D. M., and J. R. Glastonbury, "Particle-Liquid Hydrodynamics and Mass Transfer in a Stirred Vessel: II—Mass Transfer," *Trans. Inst. Chem. Eng.*, **50**, 132 (1972b).

Nienow, A. W., and R. Conti, "Particle Abrasion at High Solids Concentration in Stirred Vessels," *Chem. Eng. Sci.*, **33**, 1077 (1978).

Nienow, A. W., "The Mixer as a Reactor: Liquid/Solid Systems," *Mixing in the Process Industries*, 2nd ed., N. Harnby, M. F. Edwards, and A. W. Nienow, eds., Butterworth-Heinemann, Oxford, p. 394 (1992).

Randolph, A. D., and M. A. Larson, *Theory of Particulate Processes*, 2nd ed., Academic Press, San Diego, CA (1988).
Rice, D. A., J. R. Cobble, and D. R. Brooks, "Effects of Turbomilling Parameters on the Simultaneous Grinding and Ferric Sulfate Leaching of Chalcopyrite," Rep. No. 9351 U.S. Dept. of the Interior, Bureau of Mines, Washington, DC (1991).
Rieger, P.-G., and H.-J. Knackmuss, "Basic Knowledge and Perspectives on Biodegradation of 2,4,6-Trinitrotoluene and Related Nitroaromatic Compounds in Contaminated Soil," *Biodegradation of Nitroaromatic Compounds*, J. C. Spain, ed., Plenum Press, New York, p. 1 (1995).
Shacham, M., and M. B. Cutlip, *POLYMATH*, The CACHE Corp., Austin, TX (1994).
Tuovinen, O. H., "Biological Fundamentals of Mineral Leaching Processes," *Microbial Mineral Recovery*, H. L. Ehrlich and C. L. Brierley, eds., McGraw-Hill, New York, p. 55 (1990).
U.S. EPA, "J.R. Simplot ex-situ Anaerobic Bioremediation Technology: TNT," *SITE Technol. Capsule*, EPA Rep. 540/R-95/529a, Cincinnati, OH (1995).

Manuscript received Sept. 15, 1999, revision received Sept. 11, 2000.